[Frontiers in Bioscience 7, d1464-1474, June 1, 2002]

THREE-DIMENSIONAL RECONSTRUCTION OF RYANODINE RECEPTORS

Terence Wagenknecht[1,2] and Montserrat Samsó [1]

[1]Biggs Laboratory, Wadsworth Center, New York State Department of Health, Albany, NY 12201, [2]Department of Biomedical Sciences School of Public Health, State University of New York at Albany, Albany, NY 12201

TABLE OF CONTENTS

1. ABSTRACT

Nearly all available information on the three-dimensional structure of the ryanodine receptor (RyR) class of intracellular calcium release channels has come from electron microscopy. This review focuses on results that have been obtained by cryo-electron microscopy of purified, detergent-solubilized receptors in combination with single-particle image processing. This approach has led to the most detailed 3D models of RyRs, which are currently at resolutions of 20-30 Å. All three of the known genetic isoforms show essentially identical architectures at this resolution: a large, 4-fold symmetric, cytoplasmic assembly that accounts for greater than 80% of the receptor's mass and is composed of at least 10 discrete, loosely packed domains, and a transmembrane region whose dimensions lead us to conclude that very little of RyR's protein mass is present on the lumenal side of the sarco/endoplasmic reticulum. Three-dimensional reconstructions determined for RyRs that have been exposed to conditions that promote either open or closed

states show subtle differences, some of which are located in the cytoplasmic assembly, at sites more distant than 100 Å from the ion channel in the transmembrane region. Several of the ligands (FK506-binding protein, calmodulin, dihydropyridine receptor) that interact *in vivo* with the skeletal RyR have been, or are in the process of being, mapped to various locations on the cytoplasmic assembly.

2. INTRODUCTION

Ryanodine receptors (RyRs), which comprise a class of intracellular calcium channels, are the largest ion channels known. In mammals, RyRs are homotetramers of net molecular mass 2.2-2.3 X 10^6 Daltons, the precise value depending on the particular genetic isoform, of which three have been characterized (1, 2). Isoform 1 (RyR1) is highly enriched in skeletal muscle, isoform 2 (RyR2) is enriched in cardiac muscle, and isoform 3 (RyR3), as well as RyR1 and RyR2, are found at lower levels in a variety of tissues.

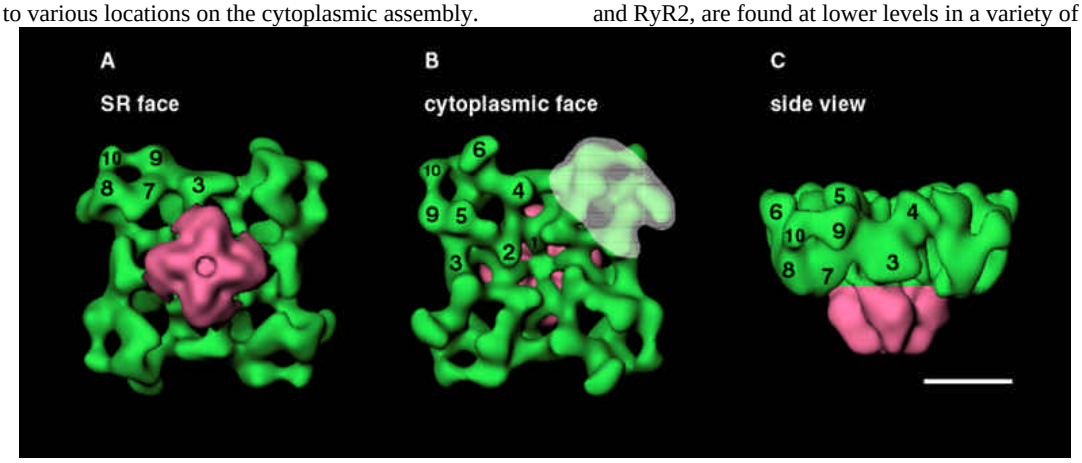

Figure1. Three-dimensional architecture of RyR1. Solid body representations of RyR1 determined by cryo-electron microscopy and 3D reconstruction. The cytoplasmic assembly is shown in green and the transmembrane region is in pink. Numerals have been assigned to each of the domain-like structures that comprise the cytoplasmic assembly. Three orientations are shown. (**A**) View onto the SR face. This surface contains the transmembrane region. (**B**) View onto the opposite face from that in (A). This is the surface that would interact with the T-tubule in skeletal muscle. The white shadowing indicates one of the four equivalent areas with high probability of interaction with the DHPR. (**C**) A side view, obtained by rotating the views in (A), (B) by 90º about the horizontal. Scale bar, 100 Å. Adapted from (13).

Being both very large and integral membrane proteins, RyRs present special challenges to the determination of their three-dimensional structures. Probably the method of choice for detailed structural characterization of RyRs would be X-ray crystallography, but this technique requires highly ordered crystals, which are not easily obtained for membrane proteins or for large protein assemblies. Furthermore, in striated muscle, and possibly in other tissues as well, RyRs form specific interactions with other proteins to form gigantic signal-transducing assemblies of such complexity that there is little hope of isolating them, much less of determining their structure at the atomic level.

In the past decade, cryo-electron microscopy (cryo-EM) of isolated macromolecules, in conjunction with computerized single-particle image processing, has emerged as a powerful methodology for determining the three-dimensional structures of large, multi-component proteins and ribonucleoproteins (3-7). Cryo-EM has eliminated the artifacts associated with chemical fixation, dehydration, and contrast enhancement by heavy metals that have plagued EM in the past, but it has necessitated averaging large numbers of images to compensate for the low signal-to-noise ratio inherent in micrographs of native, ice-embedded proteins (8). Unlike other structural techniques where "smaller is better," this approach is best suited for large assemblies of macromolecules. Probably its most appreciated advantages are that crystals are unnecessary and that rather small quantities of specimen are required (e.g., less than a microgram of protein is required to make a single grid, which can provide sufficient data to determine a 3D structure to moderate resolution). The main limitation of the approach is that atomic resolution, although possible in principle, is difficult to attain, and for studies of RyR, the best resolution to date is 20 Å (9) and most published studies report resolutions of about 30 Å.

In this review we summarize the major findings thus far in elucidating the 3D structure of RyRs by cryo-EM and single-particle image processing. For readers who

desire more details on the methodology, as it pertains to RyRs, a recent review is recommended (10).

3. BASIC FEATURES OF RYR ARCHITECTURE

The first 3D reconstructions from micrographs of frozen-hydrated, detergent-solubilized RyR1s were reported in the mid 1990s by our laboratory (11) and independently by another group at the Baylor College of Medicine (12). All subsequent studies to date that have applied 3D cryo-microscopy techniques to RyRs have been produced by these same two laboratories, which we will henceforth refer to as the Albany and Baylor groups when it is necessary to distinguish them. The initial reconstructions from the two groups, which were obtained by somewhat different methods (outlined in (13)), had an estimated resolution of ≈ 30 Å and, reassuringly, showed nearly identical structural features. A surface representation of the 3D model of Radermacher *et al.* (11) is illustrated in Figure 1 from which it is apparent that RyR has two main structural components: (a) a larger structure having a convoluted substructure and the overall shape of a square prism (280 X 280 X 120 Å), and (b) projecting from one of its faces, a smaller, 4-fold symmetric structure that appears more solid and less complex in appearance. The larger of these represents the cytoplasmic region of the receptor, whereas the smaller represents the transmembrane portion. The assignment of these cytoplasmic and transmembrane regions is based, in part, from the appearance of RyRs in electron micrographs of specimens in which the receptors remain integrated in their natural membrane environment (e.g. 14, 15). The clear fourfold symmetry is consistent with the receptor being a tetramer.

3.1. Cytoplasmic Assembly/Region

The cytoplasmic assembly of RyR1 appears to consist of 10 or more discrete globular domains per subunit that are clearly resolvable due to their separation by solvent-accessible regions. Reassuringly, the arrangement of the various domains, as illustrated by Figure 1, in which each domain has been assigned arbitrarily a numeral (Albany group), is essentially identical in all of the reconstructions that have been reported thus far. The four "3" domains, which form the sides of the square slab defined by the cytoplasmic assembly, are the largest of the domains, and the Baylor group has assigned to them a special name, the "handles". A cluster of domains (numbered 5-10) forms each of the corners of the cytoplasmic assembly, and the Baylor group has named these assemblages, the "clamps". The four "2" domains surround a central 40-50 Å diameter solvent-filled pocket that appears to extend to the proximal surface of the transmembrane region. Domain 1 appears to connect the cytoplasmic and transmembrane structures. Each clamp is connected to the remainder of the receptor via three interactions: (i) between domains 5/9 of the clamp and one of the handles, (ii) between clamp domain 6 and domain 4 which in turn attaches to the other handle, and (iii) between clamp domain 5 and domain 2.

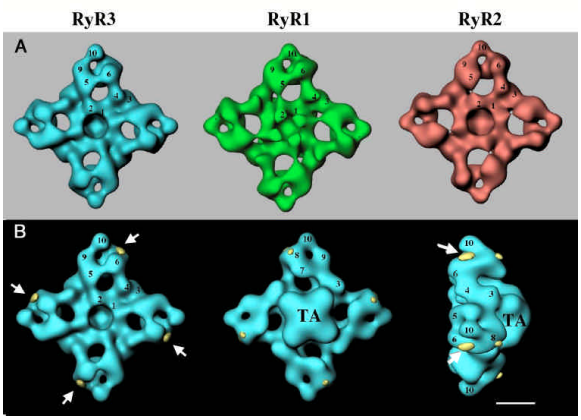

Figure 2. Comparison of 3D reconstructions of RyR1, RyR2, RyR3. (**A**) Shows solid body representations of RyR3 (blue), RyR1 (green), RyR2 (red) viewed onto the cytoplasmic surface. Note conservation of domain architecture. (**B**) RyR3 superimposed with the major differences (yellow) that are obtained when the 3D reconstruction of RyR3 is subtracted from that of RyR1. Arrows indicate the main difference which is tentatively attributed to the D2 region which is absent from RyR3 (see text for details). Adapted from (28).

We emphasize that the subunit boundaries cannot be discerned in the 3D reconstructions (i.e., it is not clear how to apportion the 4 sets of 10 domains to each of the four subunits). It is highly likely, however, that the entire cytoplasmic region is formed from amino acid residues beginning at the amino-terminus and extending to residues 4,000-4,500. The remainder of the 5,037 residues that comprise the RyR1 subunit form the transmembrane region.

3.2. Transmembrane assembly/region

When viewed along the 4-fold symmetry axis and onto the face that contains it (Figure 1A), the transmembrane region appears square in overall shape, but it is rotated by about 40 degrees from the square outlined by the cytoplasmic assembly. When RyR1 is viewed from

the side (Figure 1C), the transmembrane region frequently appears tapered, with the end that is connected to the cytoplasmic region having a larger diameter, ≈120 Å, than the other end. The transmembrane assembly's length is about 70 Å, more than sufficient to traverse a membrane bilayer. The shape of the transmembrane region varies between independently determined reconstructions. As will be seen below, some of this variability is likely due to differing functional states of the receptor, but other uncharacterized factors are also involved. One possibility, for which there is some evidence (unpublished observations, Albany group), is that the transmembrane assembly's orientation with respect to the cytoplasmic assembly varies among the receptors that contribute to a reconstruction, resulting in this part of the reconstruction being less reliably resolved in some reconstructions.

In some 3D reconstructions of RyRs a 20-30 Å-diameter column of low density (indicating solvent accessibility) extends along the 4-fold symmetry axis of the transmembrane region (e.g., Radermacher et al. (11)). When treated with ryanodine, which according to functional analyses locks the receptor in an open or partially open state, this region becomes better defined, and it appears to form a channel across the transmembrane region (16). It has been argued that this channel corresponds to the wider regions of the ion-conducting pathway of RyR1. This argument is supported by analogy to the known structure of the potassium channel from *Streptomyces lividans* (17), which is also a tetramer and may be structurally homologous to RyR in the region of the transmembrane pore (18-20).

We suggest that the location of the ion-conducting pore or pores should be regarded as an open question, and that alternative "multi-barreled" models cannot be excluded at present (21). The single-pore model does not readily account for the four discrete, evenly spaced subconductance states that numerous laboratories have observed for RyR1 and RyR2 (22, 23). Possibly, four independent (but allosterically coupled) pores are present in the transmembrane region but are not resolvable at the resolutions attained in 3D reconstructions, and the centrally located low-density region is either not involved in ion conduction or represents only part of a pathway that branches to form four "subpores". It is worth remarking that the recently determined atomic models for aquaporin family members, also homotetramers, reveal functional transport pathways in each of the subunits, and a larger, centrally located gap between the four subunits that is not involved in transport (24-26). Finally, some recent reconstructions of RyR1 determined in our laboratory show low-density substructure in the transmembrane region that could be consistent with four pores per receptor (27).

4. COMPARISON OF RYR ISOFORMS

Not surprisingly, given the >60% sequence identity among the three mammalian RyR isoforms, 3D reconstructions of RyR2 and RyR3 (Figure 2A, left and right panels) are nearly identical to that of RyR1 (Figure2A, middle panel) in the 30-40 Å resolution range

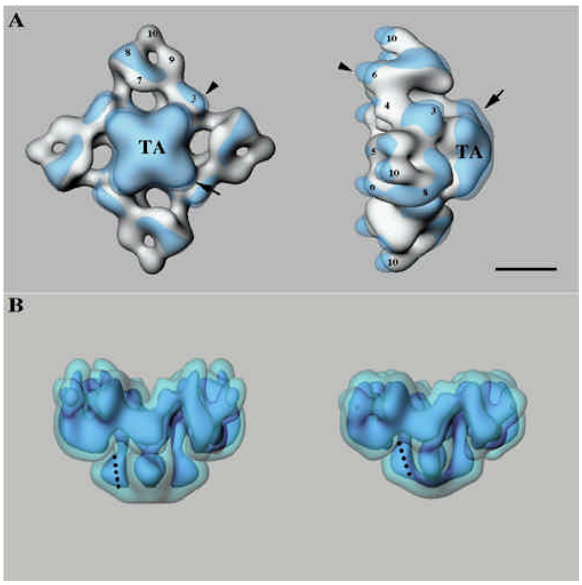

Figure 3. Comparison of putatively open and closed states of RyR3. (**A**) Solid body representation of closed RyR3 depicted in solid gray with open RyR3 superposed in transparent blue. Arrows denote regions where the surface of open RyR3 extends significantly beyond the surface of closed RyR3. (**B**) Open RyR3 (left) and Closed RyR3 (right) displayed at two density thresholds. The higher threshold (solid, darker blue) illustrates how the mass density shifts between the open and closed forms, particularly in the transmembrane region. Dotted line indicates an elongate region of density that splays outward in the open relative to the closed states. Scale bar, 100 Å. Adapted from (28).

(28, 29). RyR3 differs significantly from RyR1 in a region at the distal edge of domain 6 (Figure 2B) at each of the clamps. This difference corresponds to ≈10 kDa of protein mass that is present in RyR1 but absent in RyR3. Intriguingly, the sequence of RyR3 shows a deletion of 104 residues (1303-1406) relative to RyR's sequence. Thus, it seems likely that domain 6 bears this region of the sequence, which has been referred to as divergency region 2 (D2), one of three regions within RyR sequences that is highly variable among the three isoforms (30).

5. CONFORMATIONAL STATES OF RYR1 AND RYR3

Functional studies have established that open conformations of RyR1 are favored by the presence of Ca^{2+} (optimal at about 0.1 mM) and millimolar ATP. Channel closing is favored by the absence of nucleotide and submicromolar Ca^{2+}. The plant alkaloid ryanodine, binding to its high (nanomolar) affinity site, locks the receptor in an open state whose conductance is ≈40% that of the open state achieved with Ca^{2+} and nucleotide. The Baylor group compared a 3D reconstruction of RyR1 determined under conditions that favor the closed state with that obtained in the presence of ryanodine (16). Subsequently, reconstructions of RyR1 in the presence of activating levels of Ca^{2+} and nucleotide were reported (31), and more

recently the Albany group has determined 3D models of RyR3 under similar conditions (28). A caveat to all these studies is that they were performed on detergent-solubilized receptors, whereas functional gating analyses of the receptors are necessarily done on receptors in their native bilayer environment. Cryo-EM and 3D reconstruction of bilayer-associated RyRs have thus far not been feasible.

Reassuringly, the differences between the 3D reconstructions of the putatively open and closed states of the RyR1 (31) are remarkably similar to those reported for RyR3 (28). The results obtained for RyR3 are shown in Figure 3. In Figure 3A, the closed form is shown as a solid gray-colored body, and the open form is superimposed in transparent blue. Thus, wherever the receptor appears blue in color, the structure of the open form is outside of the envelope defined by the closed form; conversely where the receptor is gray, the envelope of the closed form is outside of that of the open form. In Figure 3B, the open (left) and closed (right) structures are shown simultaneously at two density threshold levels: a semitransparent blue defines the molecular boundaries, and a higher threshold in a darker shade of blue is used to better reveal the nature of the structural differences between the two states, particularly in the transmembrane region.

The following are regarded as the most significant differences between open and closed RyR3 and RyR1:

1. The transmembrane assembly appears to rotate about the fourfold symmetry axis by a few degrees for RyR3 (Figure 3A). This was seen for RyR1 in the ryanodine-induced open state, but it was not evident in the Ca^{2+} /nucleotide-induced open state.

2. Columnar regions of high density within the transmembrane region appear to splay apart in the open relative to the closed states (dotted lines in Figure 3B), thereby creating a lower density running down the center of the transmembrane region. This effect was strongest for the ryanodine-modified RyR1. As discussed earlier, this region may or may not represent the pathway followed by ions when the receptor opens.

3. The transmembrane region is slightly taller when viewed from the side in the open vs. closed state (Figure 3A, rightmost arrow in right panel)

4. In the clamps, the height of domains 6 and 10 appear to increase in height by ≈15 Å.

5.A slight weakening of the density that connects domains 9 and 10 occurs in the open relative to the closed state. This effect is more apparent in the RyR1 reconstructions than in those of RyR3, and it is not clear in Figure 3.

Most unexpected among the differences between open and closed RyRs were the changes in the clamps, which are separated by well over 100 Å from some of the changes that occur in the transmembrane region. As is discussed in more detail below, the clamps are likely involved in interactions between the dihydropyridine

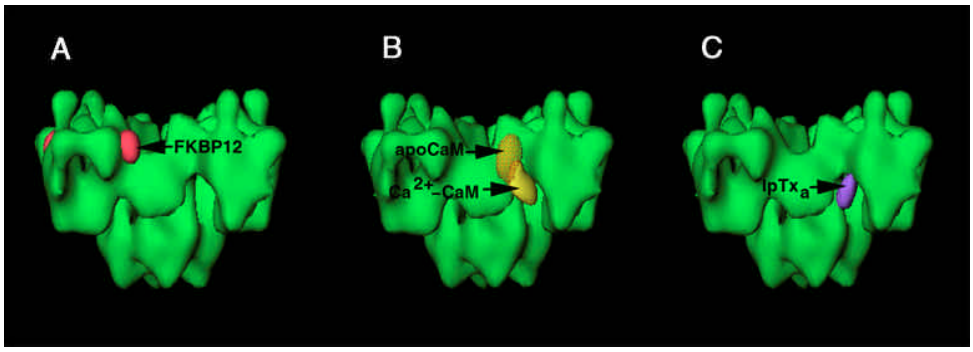

Figure 4. Ligand binding locations on RyR1. (**A**) Location of FKBP12 (fuchsia). (**B**) Location of both forms of CaM: apoCaM (transparent orange) and Ca^{2+}-CaM (solid yellow) (**C**) Location of $IpTx_a$ (purple). The three 3D difference maps are superposed onto a common 3D reconstruction of RyR1 in absence of any ligand.

receptor (DHPR) and RyR1 that appear to be essential for excitation-contraction (E-C) coupling in skeletal muscle (32). The changes in the clamp structure that accompany channel gating may be related to this communication between the two receptors.

6. INTERACTION SITES OF RYR MODULATORS

A major application of 3D cryo-EM is to characterize the modes of interaction between macromolecular assemblies and the proteins with which they functionally interact *in situ*. Among the ligands of RyR1 are the 12-kDa FK506-binding protein (FKBP12), calmodulin, the dihydropyridine receptor, calsequestrin, and the two integral membrane proteins of the sarcoplasmic reticulum (SR), triadin and junctin (33). The Albany group has investigated complexes of RyR1 with FKBP12, calmodulin, and an analog of the DHPR. The experiments are conceptually very simple: RyR and ligand are mixed *in vitro* under conditions favoring complex formation, the mixture is diluted if necessary, and then applied to specimen grids and frozen for EM in the usual way. If necessary, a control reconstruction is done of RyR lacking the ligand but otherwise identical. Finally, the reconstructions of the RyR with and without ligand are quantitatively compared by subtracting the corresponding voxels of the control from the experimental reconstruction to generate a 3D difference map.

6.1. FKBP12

FKBP12 is a *cis-trans* prolyl isomerase that binds with high affinity to RyR1 (34). Four copies of FKBP12 are bound per RyR1 tetramer and they can be induced to dissociate upon addition of either of the immuno-suppressant drugs, rapamycin or FK506 (35). Loss of FKBP12 appears to destabilize the closed state of RyR1 (36, 37), but the role of FKBP12 *in vivo* is uncertain. Marks and co-workers found evidence that FKBP12 is involved in mediating interactions between RyR1s, which form arrays in their native environment in muscle (38), and there is also evidence that FKBP12 plays a role in E-C coupling. RyR2 also binds FKBP12 or a close relative, FKBP12.6 (39), and RyR3 has been reported to bind FKBP12 (40, 41), although the functional effects, if any, on these isoforms are not clearly defined at present. A more detailed treatment of the FKBP:RyR2 interaction can be found elsewhere (A. Marks, 2002) in this volume.

Initial attempts to determine the FKBP12 binding site on RyR1 by our laboratory failed to detect any loss of protein mass from isolated RyR1 following treatment with the drug FK506. Apparently, the isolated RyR1 was deficient in bound FKBP12 because if FKBP12 was added exogenously to RyR1 in the presence and absence of FK590 (equivalent to FK506), then a highly significant difference was found that corresponded to excess mass in the non-drug-treated receptors (42, 43). The volume of the difference was consistent with that expected for a 12-kDa protein. Figure 4A shows that this density, which is attributed to FKBP12, is located adjacent to domain 9 where it joins to domain 3 (handle). Although no significant conformational changes in RyR1 were discernible at the rather limited resolution that was attained in this study, apparently such changes must not only occur, but they must be far-reaching. This is because the binding location of FKBP12 is about 120 Å from the center of the transmembrane region, which contains the ion-conducting pore (or pores) that is (are) modulated by FKBP12.

6.2. Calmodulin

As mentioned in Section 5, RyR is regulated by Ca^{2+}. In addition, RyR is further modulated by CaM, another protein that is also regulated by Ca^{2+}. CaM's structure and function depends on whether Ca^{2+} is bound to each of its two modules (44, 45). These two forms of CaM exert opposite effects on the RyR. At submicromolar Ca^{2+}, CaM (apoCaM) activates partially RyR1, whereas at millimolar Ca^{2+}, Ca^{2+}-CaM becomes a partial inhibitor (46-49). In the Albany laboratory we have localized this 16-kDa protein on the surface of RyR1, both at millimolar and submicromolar [Ca^{2+}], by 3D difference mapping. Both types of CaM bind to the cytoplasmic assembly, with a stoichiometry of one CaM per RyR1 subunit, in agreement with current biochemical determinations (50). However, depending on the Ca^{2+} concentration, CaM localizes at slightly different sites. Ca^{2+}-CaM binds within the crevice formed by domains 3 and 5/6 (51, 52), and apoCaM binds to the external part of domain 3 (53) (Figure 4B). The distance between the centers of the binding sites is 33 ±5 Å, with a small area of overlap. This observed overlap is consistent with the protection found for two trypsin cleavage sites (after residues 3630 and 3637) by either form

of CaM (50). In addition, recent results using synthetic peptides and single-point RyR1 mutants have shown that the two forms of CaM bind to very close, but distinct sites (54, 55). The separation between binding sites that we found is somewhat larger than one would expect from the separation in sequence (about 5 residues). This apparent discrepancy can be reconciled by taking into account the multiple binding possibilities of both CaM modules, e.g. as discussed in (53), by a RyR1 conformational change involving the CaM target sequence, or by a combination of both. The proximity of both CaM binding sites might support switching of the CaM molecule between them under the successive Ca^{2+} cycles without necessity of complete dissociation from the RyR1, thus allowing a faster response.

6.3. Dihydropyridine receptor

The interaction of RyR with the DHPR deserves special attention because of the key role it plays in E-C coupling in striated muscle. Within myofibers, specialized regions termed calcium release units (CRUs) occur where the terminal cisternae of the SR, which contains the RyRs, and tubular invaginations (T-tubules) of the plasma membrane, which contain the DHPRs, are close to each other (56); Protasi, elsewhere in this volume). The close association of DHPRs and RyRs permits the activation of the latter by the former in a process known as E-C coupling. A similar functional coupling between RyR and DHPR has also been found in neurons (57, 58).

It is widely believed that in skeletal muscle E-C coupling occurs by a mechanical coupling mechanism (59, 60), whereby depolarization of the cell membrane/T-tubule induces a conformational change in the DHPR, which causes additional conformational changes in the RyR1 as a result of direct interactions between the two. Electron microscopy of freeze fracture replicas revealed that CRUs in skeletal muscle consist of ordered, complementary arrays of RyR1 and DHPR (14, 61, 62). Groups of four DHPRs (tetrads) appear to match alternate RyR1s. The relative geometry of the two proteins suggests that the clamps of RyR1 (see white shadowed area in Figure 1B) are most likely to be involved in this interaction with DHPRs (13).

DHPR, an L-type Ca^{2+} channel, is a heteromer of 5 different subunits ($\alpha1$, $\alpha2$, β, δ, γ) (63). The ion-conducting pore and voltage sensor functions are supported mainly by the $\alpha1$ subunit, which contains 4 homologous repeats each with 6 predicted transmembrane domains. The three-dimensional structure of $\alpha1\beta$ complexes, as determined by EM and 3D reconstruction, is characterized by an elongate shape of 12 nm height and 9-10 nm width, with a central hole (64). Heart and skeletal muscle have distinct isoforms of $\alpha1$, and the cytoplasmic loop between the second and third transmembrane repeats (II-III loop) is specially important in mediating the interaction between RyR and DHPR as well as in determining the type of E-C coupling (skeletal or cardiac) (65). Other cytoplasmic regions of the DHPR are probably also involved in the interaction with RyR1 (66, 67). The II-III loop contains functionally distinct subdomains, with activating and inhibiting activities (68, 69). Efforts to map more precisely the DHPR:RyR1 interaction have been hampered by the low affinity between these two proteins, and use of fixatives has found only moderate success (70).

The Albany group has used Imperatoxin A ($IpTx_a$), a high affinity peptide mimetic of the activating region of DHPR's II-III loop (amino acid residues 666-791) (71), to begin mapping the RyR sites that interact with the DHPR (72). $IpTx_a$ mimics a region near the N-terminus of the II-III loop that contains a cluster of basic residues. This 33-residue peptide toxin enhances binding of ryanodine to the receptors (73), and induces long-lived subconductance states (71, 74). Cryo-electron microscopy and image processing of streptavidin-labeled $IpTx_a$ incubated with RyR1 showed that $IpTx_a$ binds to the base of the crevice delimited by domains 3 and 7/8 of the cytoplasmic assembly (Figure 4C). The relatively large distance of the $IpTx_a$ binding site from the putative ion channel (~110 Å) is indicative of an allosteric mechanism for activation of calcium release. The distance between the centers of mass of neighboring $IpTx_a$s is 150 Å, a distance that is compatible with the distance between neighboring DHPRs of a tetrad in the triad junction (14). When RyR1 is viewed from the side (Figure 4C), $IpTx_a$ locates almost 5 nm from the T-tubule-face of RyR1. For the basic sequence of the II-III loop to reach this region would apparently require a fully extended conformation for the first 15 residues of the II-III loop that precede it (68). $IpTx_a$ is discussed in more detailed by Valdivia, et al (2002) in this volume.

An intriguing feature comes from the comparison of the $IpTx_a$ binding site (Figure 4C) with that of both CaM binding sites (Figure 4B). In particular, the binding site for $IpTx_a$ is very close to that for Ca^{2+}-CaM. If indeed $IpTx_a$ is a marker of the DHPR's II-III loop:RyR1 interaction, then CaM might play a direct role in the E-C coupling interaction.

Two additional results from 3D cryo-EM implicate RyR1's clamps as being involved in binding DHPR. Recall that the D2 region (RyR1 residues 1302-1404), which may be involved in the DHPR:RyR1 interaction (75), was assigned to domain 6, which is found in the clamps (section 5, Figure 2B, Figure 5). Finally, our laboratory has begun to characterize the interaction of RyR1 with a cloned full-length II-III loop peptide (76), and preliminary results from cryo-EM are consistent with the II-III loop binding to a location near that assigned to the D2 region (77).

7. CORRELATION OF RYR1's AMINO ACID SEQUENCE WITH ITS 3D ARCHITECTURE

An atomic structure for RyR seems not to be forthcoming, but even at the resolutions currently being attained by 3D cryo-EM it is feasible to determine the locations of surface-exposed amino acids if they can be appropriately labeled. With a sufficient number of amino-acid localizations it should be possible to largely define

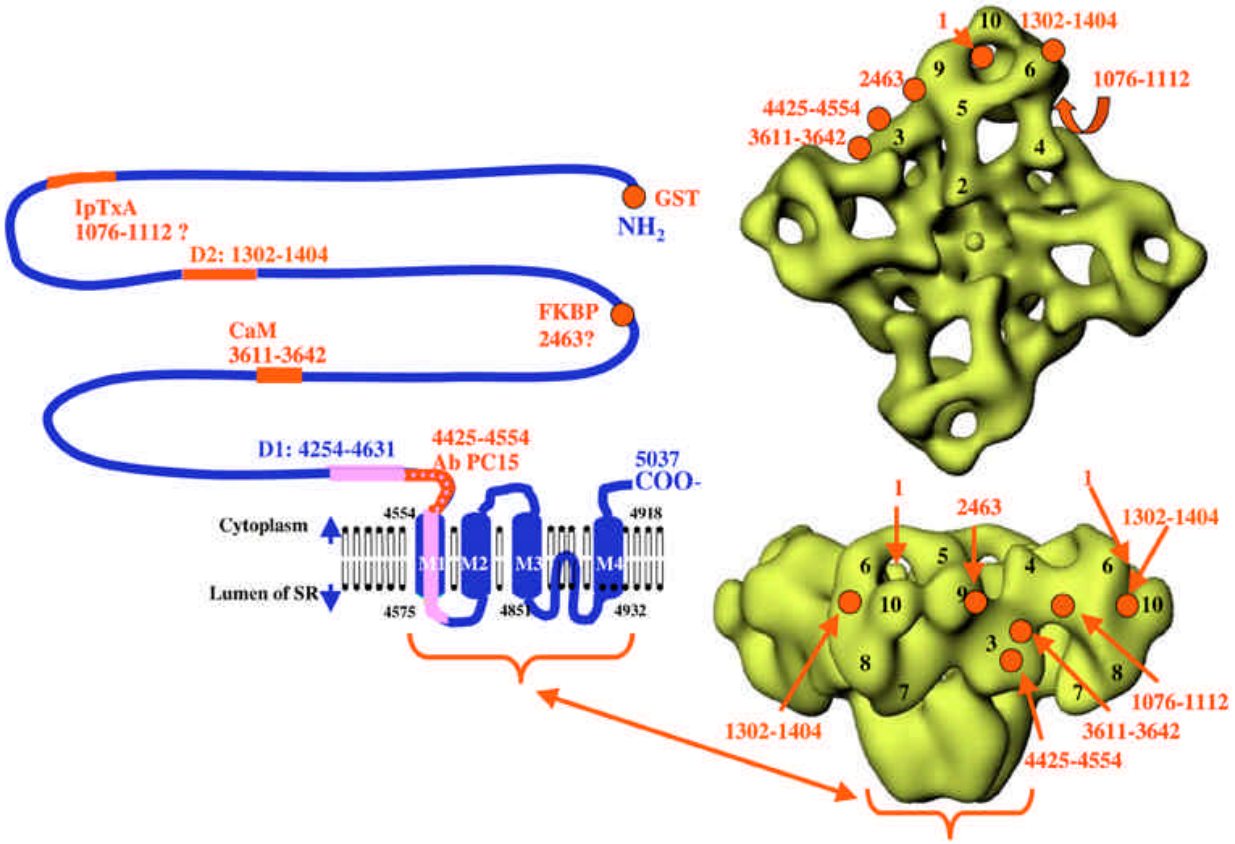

Figure 5. Sequence-structure correlation for RyR1 (tentative). Left side shows schematic representations of RyR1 sequence. Four transmembrane segments and a luminal loop between M3 and M4 that might form part of the ion pore are shown as proposed by Balshaw et al. (18), but the actual number of transmembrane segments may be greater than 4. Regions highlighted by red segments or dots are proposed to be involved in binding ligands that have been localized by 3D cryo-EM. The name of the ligand is also indicated in red, adjacent to the residue numbers. Question marks indicate assignments that are most speculative. Right side shows solid body representations of RyR1 in cytoplasmic and side views. The locations of the sequence-specific markers are indicated in red. The transmembrane region is bracketed and its relation to the sequence indicated by the double-headed red arrow. See text for references and details.

how the 5,037 amino acids that comprise the RyR1 subunit are apportioned among the various domains that are resolved in the 3D reconstructions. Even at this level of detail, it will in some cases be possible to evaluate the plausibility of hypothesized functions for particular amino acids from biochemistry experiments. For instance, amino acids of RyR1 that are proposed to interact directly with a ligand (e.g. calmodulin) should map to a spatially restricted region on the surface of the receptor that coincides with the location where the ligand itself is found to bind. If in the future high resolution structures are determined for cloned, expressed fragments of the RyR subunit, then having one or a few of a fragment's amino acid residues mapped on the receptor's surface by 3D cryo-EM will facilitate fitting the atomic model of the fragment into low-resolution density maps of the intact receptor.

An antibody of known specificity for a particular region of the RyR sequence would be a suitable probe for 3D cryo-microscopy. Although a number of sequence-specific antibodies have been described, our experience has been that many do not bind with sufficient affinity to detergent-solubilized RyRs for cryo-EM. A monoclonal antibody raised against an expressed fusion protein containing residues 4426-4621 of RyR1 (78) was found by 3D cryo-EM to bind on domain 3, near the transmembrane region (79). As indicated in figure 5 the antibody most likely recognizes an epitope contained within the amino-terminal half of the fusion protein.

For several of the ligands that were described in section 6, the amino acid residues of RyR that are involved in binding them are either known or plausible assignments have been made. Thus, these ligands can serve as sequence-specific probes. Calmodulin, for example, has been shown by two groups to bind at or very near to Cys-3635 of RyR1 (54,80). The interaction site for FKBP12 has been mapped to amino acid residues in the immediate vicinity of Pro-2463, although another study implicated a site contained within residues 2756-2803 of RyR1 (41).

More speculative is the site on RyR1 recognized by $IpTx_a$. If $IpTx_a$ is indeed a mimic of the DHPR's II-III loop, then RyR1 residues 1076-1112 may be involved in the interaction (81). These localizations are summarized in Figure 5.

The D2 region (RyR1 residues 1302-1404) is also tentatively indicated in Figure 5. This assignment was made on the basis of the comparison of the RyR1 and RyR3 reconstructions discussed earlier (see also Figure 2). Recall that the D2 region is missing from the RyR3 sequence, and so we interpreted the excess mass that was present in the reconstruction of RyR1 relative to that of RyR3 as corresponding to this region of RyR1's sequence.

Finally, the location of the N-terminus of RyR1 was inferred to be near the center of the clamp (Figure 5) from a 3D reconstruction of cloned, expressed RyR3 that contained glutathione transferase fused at the N-terminus (82). In the future, molecular cloning techniques that introduce modifications (e.g. insertions) at internal regions of the RyR sequence may result in an efficient, comprehensive protocol for determining the locations of surface-exposed segments of the receptor's sequence.

Most of the sequence assignments indicated in Figure 5 should be regarded as tentative. As more sequence-specific probes are mapped, it will be possible to refine the assignments. Nevertheless, even with the limited data available, a self-consistent model is emerging. It appears that the amino terminal region of the RyR1 subunit, residues 1-1,400 at minimum, form each of the clamps (domains 5-10). The handle (domain 3) contains residues from the middle of the sequence (3,600- 4,400). Independent evidence from various sources has established that probably all of the transmembrane segments are contained within the 500-1000 carboxy-terminal amino acid residues (recently reviewed by Williams et al. (20).

8. PERSPECTIVE

8.1. High-resolution

The necessity of a high-resolution structure to gain a full understanding of how RyRs function cannot be understated. Efforts to obtain crystals of intact RyRs suitable for X-ray crystallography may require years before success is achieved. Electron crystallography, which requires two-dimensional crystals, could also yield a high-resolution structure for RyR, but the 2D crystals that have been obtained thus far show diffraction only to ≈25 Å resolution (83).

Whereas cryo-EM and single-particle image processing techniques can in principle achieve atomic resolution, this has not yet been achieved in practice. Currently, the highest resolution reported using these techniques for complexes that lack high symmetry is 7.5 Å, which was obtained for a 50S ribosomal subunit (84). Since the first 3D reconstructions of RyR1 were reported in 1994 (11), the resolution of reported reconstructions has only improved from 30 Å to about 20 Å (Wah Chiu, Baylor School of Medicine, personal communication). It is not clear why the pace of progress has not been faster, but one possibility is that there is some intrinsic disorder in the RyR molecules which could be remedied by modifying the sample preparation techniques currently being used.

An alternative strategy to achieve atomic resolution is to crystallize and solve the atomic structures of cloned, expressed polypeptides corresponding in sequence to continuous segments of the RyR amino-acid sequence. Methods have been developed, and are continually improving, for fitting atomic models of component proteins into medium resolution maps obtained by 3D cryo-microscopy of the complexes containing them (85-87). If structures from a sufficient number of RyR-derived fragments could be obtained by X-ray crystallography or NMR techniques, and docked into RyR 3D maps, then a determined in this piecemeal manner. Thus far crystallization of only one RyR1 fragment, corresponding to a portion of the D2 regions (see Figure 5), has been reported (88).

8.2. 3D localization of functional/structural sites

The recent demonstration by Liu *et al.* (83) that structurally intact, genetically modified RyRs can be isolated from transfected cultured cells should greatly accelerate the rate of progress in determining the locations of functional/structural sites by 3D cryo-EM. Of the many possible modifications that might prove useful for this purpose, the one that we are currently testing involves introducing into the RyR sequence an insertion of amino acids that form an epitope for a commercially available monoclonal antibody. If the epitope is inserted into a surface-exposed region of RyR, then the addition of the antibody (or Fab fragment) to isolated receptors should result in the formation of immunocomplexes that can be solved by cryo-EM and 3D reconstruction. It should be appreciated that the precision with which labels (e.g. Fab fragments) can be positioned in the 3D density maps is several-fold greater than the resolution of the reconstruction itself; that is to say, epitope localizations with a precision approaching 10 Å should be achievable even at ≈30 Å resolution, which is routinely attained for RyRs.

9. ACKNOWLEDGMENT

Supported by the National Institutes of Health R01AR40615, RR01219, and by the Muscular Dystrophy Association.

10. REFERENCES

1. Franzini-Armstrong,C. & Protasi,F. Ryanodine receptors of striated muscles: a complex channel capable of multiple interactions. *Physiol. Rev.* 77, 699-729 (1997)

2. Ogawa,Y., Kurebayashi,N. & Murayama,T. Ryanodine receptor isoforms in exciation-contraction coupling. *Advances In Biophysics* 36, 27-64 (1999)

3. Frank,J. Three-Dimensional Electron Microscopy of Macromolecular Assemblies. Academic Press, New York (1996)

4. Baumeister,W. & Steven,A.C. Macromolecular electron microscopy in the era of structural genomics . *Trends Biochem. Sci.* 25, 624-631 (2000)
5. Chiu,W., McGough,A., Sherman,M.B. & Schmid,M.F. High-resolution electron cryomicroscopy of macromolecular assemblies. *Trends in Cell Biology* 9, 154-159 (1999)
6. Frank,J. Cryo-electron microscopy as an investigative tool: the ribosome as an example . *BioEssays* 23, 725-732 (2001)
7. Nogales,E. & Grigorieff,N. Molecular machines: Putting the pieces together . *J. Cell Biol.* 152, F1-F10 (2001)
8. Dubochet,J., Adrian, M., Chang, J.-J., Homo, J.-C., Lepault, J., McDowall, A. W., & Schultz, P. Cryo-electron microscopy of vitrified specimens. *Quart. Rev. Biophys.* 21, 129-228 (1988)
9. Serysheva,I.I., Ludtke,S.J., Hamilton,S.L. & Chiu,W. Structure of skeltal muscle calcium release channel by electron cryomicroscopy: approaching high resolution. *Biophys. J.* 78, 485A (2000)
10. Orlova,E.V., Serysheva,I.I., Hamilton,S.L., Chiu,W. & van Heel,M. In: The structure and function of ryanodine receptors, 24-46. Eds: Sitsapesan,R. & Williams,A.J., Imperial College Press, London, UK (1998)
11. Radermacher,M., Rao, V., Grassucci, R., Frank, J., Timerman, A. P., Fleischer, S., & Wagenknecht, T. Cryo-electron microscopy and three-dimensional reconstruction of the calcium release channel ryanodine receptor from skeletal muscle. *J. Cell Biol.* 127, 411-423 (1994)
12. Serysheva,I.I, Orlova, E. V., Chiu, W., Sherman, M. B., Hamilton, S. L. & van Heel, M. Electron cryomicroscopy and angular reconstitution used to visualize the skeletal muscle calcium release channel. *Structural Biology* 2, 18-24 (1995)
13. Samso, M. & Wagenknecht,T. Contributions of electron microscopy and single-particle techniques to the determination of the ryanodine receptor three-dimensional structure. *J. Struct. Biol.* 121, 172-180 (1998)
14. Block,B.A., Imagawa,T., Campbell,K.P. & Franzini-Armstrong,C. Structural evidence for direct interaction between the molecular components of the transverse tubule/sarcoplasmic reticulum junction in skeletal muscle. *J. Cell Biol.* 107, 2587-2600 (1988)
15. Saito,A., Inui,M., Radermacher,M., Frank,J. & Fleischer,S. Ultrastructure of the calcium release channel of sarcoplasmic reticulum. *J. Cell Biol.* 107, 211-219 (1988)
16. Orlova,E.V., Serysheva,I.I., van Heel,M., Hamilton,S.L. & Chiu,W. Two structural configurations of the skeletal muscle calcium release channel. *Nature Structural Biology* 3, 547-552 (1996)
17. Doyle,D.A. Cabral, J. M., Pfuetzner, R. A., Kuo, A., Gulbis, J. M., Cohen, S. L., Chait, B. T., MacKinnon, R. The structure of the potassium channel: molecular basis of K^+ conduction and selectivity. *Science* 280, 69-77 (1998)
18. Balshaw,D., Gao,L. & Meissner,G. Luminal loop of the ryanodine receptor: a pore-forming segment? *Proc. Natl. Acad. Sci. USA* 96, 3345-3347 (1999)
19. Zhao,M., Li, P., Li, X., Zhang, L., Winkfein, R. J. & Chen, S. R. W. Molecular identification of the ryanodine receptor pore-forming segment. *J. Biol. Chem.* 274, 25971-25974 (1999)
20. Williams,A.J., West,D.J. & Sitsapesan,R. Light at the end of the Ca^{2+}-release channel tunnel: structures and mechanisms involved in ion translocation in ryanodine receptor channels. *Quart. Rev. Biophys.* 34, 61-104 (2001)
21. Marks,A.R. Cellular functions of immunophilins. *Physiol. Rev.* 76, 631-649 (1996)
22. Smith,J.S., Imagawa, T., Ma, J., Fill, M., Campbell, K. P., & Coronado, R. Purified ryanodine receptor from rabbit skeletal muscle is the calcium-release channel of sarcoplasmic reticulum. *J. Gen. Physiol.* 92, 1-26 (1988)
23. Williams,A.J. Ion Conduction and Discrimination in the Sarcoplasmic Reticulum Ryanodine Receptor/Calcium-Release Channel. *J. Muscle Res. Cell Motil.* 13, 7-26 (1992)
24. Ren,G., Reddy,V.S., Cheng,A., Melnyk,P. & Mitra,A.K. Visualization of a water-selective pore by electron crystallography in vitreous ice. *Proc. Natl. Acad. Sci. USA* 98, 1398-1403 (2001)
25. Fu,D.X., Libson, A., Miercke, L. J. W., Weitzman, C., Nollert, P., Krucinski, J. & Stroud, R. M. Structure of a glycerol-conducting channel and the basis for its selectivity. *Science* 290, 481-486 (2000)
26. Murata,K., Mitsuoka, K., Hirai, T., Walz, T., Agre, P., Heymann, J. B., Engel, A. & Fujiyoshi, Y. Structural determinants of water permeation through aquaporin-1. *Nature* 407, 599-605 (2000)
27. Samso,M. & Wagenknecht,T. Cryo-electron microscopy of the ryanodine receptor transmembrane assembly. *Biophys. J.* 80, 330A (2001)
28. Sharma,M.R., Jeyakumar,L.H., Fleischer,S. & Wagenknecht,T. Three-dimensional structure of ryanodine receptor isoform three in two conformational states as visualized by cryo-electron microscopy. *J. Biol. Chem.* 275, 9485-9491 (2000)
29. Sharma,M.R., M. R., Penczek, P., Grassucci, R., Xin, H.-B., Fleischer, S., & Wagenknecht, T. Cryoelectron microscopy and image analysis of the cardiac ryanodine receptor. *J. Biol. Chem.* 273, 18429-18434 (1998)
30. Sorrentino,V. & Volpe,P. Ryanodine Receptors - How Many, Where and Why. *Trends Pharmacol. Sci.* 14, 98-103 (1993)
31. Serysheva,I.I., Schatz,M., van Heel,M., Chiu,W. & Hamilton,S.L. Structure of the skeletal muscle calcium release channel activated with Ca^{2+} and AMP-PCP. *Biophys. J.* 77, 1936-1944 (1999)
32. Leong,P. & MacLennan,D.H. Complex interactions between skeletal muscle ryanodine receptor and dihydropyridine receptor proteins. *Biochemistry and Cell Biology* 76, 681-694 (1999)
33. Mackrill,J.J. Protein-protein interactions in intracellular Ca^{2+}-release channel function. *Biochem. J.* 337, 345-361 (1999)
34. Jayaraman,T., Brillantes, A. M., Timerman, A. P., Fleischer, S., Erdjumentbromage, H., Tempst, P., & Marks, A. R. FK506 Binding Protein Associated with the Calcium Release Channel (Ryanodine Receptor) *J. Biol. Chem.* 267, 9474-9477 (1992)
35. Timerman,A.P., Ogunbumni, E., Freund, E., Wiederrecht, G., Marks, A. R., & Fleischer, S. The calcium release channel of sarcoplasmic reticulum is modulated by FK-506-binding protein. Dissociation and reconstitution of FKBP-12 to the calcium release channel

of skeletal muscle sarcoplasmic reticulum. *J. Biol. Chem.* 268, 22992-22999 (1993)
36. Mayrleitner,M., Timerman,A.P., Wiederrecht,G. & Fleischer,S. The Calcium Release Channel of Sarcoplasmic Reticulum Is Modulated by FK-506 Binding Protein - Effect of FKBP-12 on Single Channel Activity of the Skeletal Muscle Ryanodine Receptor. *Cell Calcium* 15, 99-108 (1994)
37. Brillantes,A.B., Ondrias, K., Scott, A., Kobrinsky, E., Ondriasova, E., Moschella, M. C., Jayaraman, T., Landers, M., Ehrlich, B. E., & Marks, A. R. Stabilization of calcium release channel (ryanodine receptor) function by FK506-binding protein. *Cell* 77, 513-523 (1994)
38. Marx,S.O., Ondrias,K. & Marks,A.R. Coupled gating between individual skeletal muscle Ca^{2+} release channels (ryanodine receptors) *Science* 281, 818-821 (1998)
39. Jeyakumar,L.H., Ballester, L., Cheng, D. S., McIntyre, J. O., Chang, P., Olivey, H. E., Rollins-Smith, L., Barnett, J. V., Murray, K., Xin, H. B., & Fleischer, S. FKBP binding characteristics of cardiac microsomes from diverse vertebrates. *Biochem. Biophys. Res. Commun.s* 281, 979-986 (2001)
40. Murayama,T., Oba, T., Katayama, E., Oyamada, H., Oguchi, K., Kobayashi, M., Otsuka, K., & Ogawa, Y. Further characterization of the type 3 ryanodine receptor (RyR3) purified from rabbit diaphragm. *J. Biol. Chem.* 274, 17297-17308 (1999)
41. Bultynck,G., De Smet, P., Rossi, D., Callewaert, G., Missiaen, L., Sorrentino, V., De Smedt, H., & Parys, J. B. Characterization and mapping of the 12 kDa FK506-binding protein (FKBP12)-binding site on different isoforms of the ryanodine receptor and of the inositol 1,4,5-trisphosphate receptor. *Biochem. J.* 354, 413-422 (2001)
42. Wagenknecht,T., Grassucci, R., Berkowitz, J., Wiederrecht, G. J., Xin, H.-B., & Fleischer, S. Cryoelectron microscopy resolves FK506-binding protein sites on the skeletal muscle ryanodine receptor. *Biophys. J.* 70, 1709-1715 (1996)
43. Wagenknecht,T., Radermacher, M., Grassucci, R., Berkowitz, J., Xin, H.-B., & Fleischer, S. Locations of calmodulin and FK506-binding protein on the three-dimensional architecture of the skeletal muscle ryanodine receptor. *J. Biol. Chem.* 272, 32463-32471 (1997)
44. Finn,B.E., Evenas, J., Drakenberg, T., Waltho, J. P., Thulin, E., & Forsen, S. Calcium-induced structural changes and domain autonomy in calmodulin. *Nat. Struct. Biol.* 2, 777-783 (1995)
45. Zhang,M., Tanaka,T. & Ikura,M. Calcium-induced conformational transition revealed by the solution structure of apo calmodulin. *Nat. Struct. Biol.* 2, 758-767 (1995)
46. Yang,H.C., Reedy,M.M., Burke,C.L. & Strasburg,G.M. Calmodulin Interaction with the Skeletal Muscle Sarcoplasmic Reticulum Calcium Channel Protein. *Biochemistry* 33, 518-525 (1994)
47. Tripathy,A., Xu,L., Mann,G. & Meissner,G. Calmodulin activation and inhibition of skeletal muscle Ca^{2+} release channel (ryanodine receptor) *Biophys. J.* 69, 106-119 (1995)
48. Buratti,R., Prestipino,G., Menegazzi,P., Treves,S. & Zorzato,F. Calcium dependent activation of skeletal muscle Ca^{2+} release channel (ryanodine receptor) by calmodulin. *Biochem. Biophys. Res. Commun.* 213, 1082-1090 (1995)
49. Rodney,G.G., Williams,B.Y., Strasburg,G.M., Beckingham,K. & Hamilton,S.L. Regulation of RYR1 activity by Ca2+ and calmodulin. *Biochemistry* 39, 7807-7812 (2000)
50. Moore,C.P., Rodney, G., Zhang, J.-Z., Santacruz-Toloza, L., Strasburg, G. M., & Hamilton, S. L. Apocalmodulin and Ca^{2+} calmodulin bind to the same region on the skeletal muscle Ca^{2+} release channel. *Biochemistry* 38, 8532-8537 (1999)
51. Wagenknecht,T., Berkowitz,J., Grassucci,R., Timerman,A.P. & Fleischer,S. Localization of calmodulin binding sites on the ryanodine receptor from skeletal muscle by electron microscopy. *Biophys. J.* 67, 2286-2295 (1994)
52. Wagenknecht,T., Radermacher, M., Grassucci, R., Berkowitz, J., Xin, H.-B., & Fleischer, S. Locations of calmodulin and FK506-binding protein on the three-dimensional architecture of the skeletal muscle ryanodine receptor. *J. Biol. Chem.* 272, 32463-32471 (1997)
53. Samso,M. & Wagenknecht,T. Apocalmodulin and Ca^{2+}-calmodulin bind to neighboring locations on the Ryanodine Receptor. *J. Biol. Chem,*. in press (2002)
54. Yamaguchi,N., Xin,C.L. & Meissner,G. Identification of apocalmodulin and Ca^{2+}-calmodulin regulatory domain in skeletal muscle Ca^{2+} release channel, ryanodine receptor. *J. Biol. Chem.* 276, 22579-22585 (2001)
55. Rodney,G.G., Moore, C. P., Williams, B. Y., Zhang, J. Z., Krol, J., Pedersen, S. E., & Hamilton, S. L. Calcium binding to calmodulin leads to an N-terminal shift in its binding site on the ryanodine receptor. *J. Biol. Chem.* 276, 2069-2074 (2001)
56. Franzini-Armstrong,C., Protasi,F. & Ramesh,V. Shape, size, and distribution of Ca^{2+} release units and couplons in skeletal and cardiac muscles. *Biophys. J.* 77, 1528-1539 (1999)
57. Chavis,P., Fagni,L., Lansman,J.B. & Bockaert,J. Functional coupling between ryanodine receptors and L-type calcium channels in neurons. *Nature* 382, 719-722 (1996)
58. Fagni,L., Chavis,P., Ango,F. & Bockaert,J. Complex interactions between mGluRs, intracellular Ca^{2+} stores and ion channels in neurons. *Trends in Neurosciences* 23, 80-88 (2000)
59. Schneider,M.F. & Chandler,W.K. Voltage dependent charge movement of skeletal muscle: a possible step in excitation-contraction coupling. *Nature* 242, 244-246 (1973)
60. Rios,E. & Pizarro,G. Voltage sensor of excitation-contraction coupling in skeletal muscle. *Physiol. Rev.* 71, 849-908 (1991)
61. Franzini-Armstrong,C. & Kish,J.W. Alternate disposition of tetrads in peripheral couplings of skeletal muscle. *J. Muscle Res. Cell Motil.* 16, 319-324 (1995)
62. Protasi,F., Franzini-Armstrong,C. & Flucher,B.E. Coordinated incorporation of skeletal muscle dihydropyridine receptors and ryanodine receptors in peripheral couplings of BC_3H1 Cells. *J. Cell Biol.* 137, 859-870 (1997)
63. Catterall,W.A. Structure and regulation of voltage-gated Ca^{2+} channels. *Annual Review of Cell and Developmental Biology* 16, 521-555 (2000)
64. Murata,K., Odahara, N., Kuniyasu, A., Sato, Y., Nakayama, H., & Nagayama, K. Asymmetric arrangement of auxiliary subunits of skeletal muscle voltage-gated L-type Ca^{2+} channel. *Biochem. Biophys. Res. Commun.s* 282, 284-291 (2001)

65. Tanabe,T., Beam,K.G., Adams,B.A., Nicodome,T. & Numa,S. Regions of the skeletal muscle dihydropyridine receptor critical for excitation-contraction coupling. *Nature* 346, 567-569 (1990)
66. Leong,P. & MacLennan,D.H. The cytoplasmic loops between domains II and III and domains III and IV in the skeletal muscle dihydropyridine receptor bind to a contiguous site in the skeletal muscle ryanodine receptor. *J. Biol. Chem.* 273, 29958-29964 (1998)
67. Sencer,S., Papineni, R. V., Halling, D. B., Pate, P., Krol, J., Zhang, J. Z., & Hamilton, S. L. Coupling of RYR1 and L-type calcium channels via calmodulin binding domains. *J Biol Chem* 276, 38237-38241 (2001)
68. El-Hayek,R., Antoniu,B., Wang,J., Hamilton,S.L. & Ikemoto,N. Identification of calcium release-triggering and blocking regions of the II-III loop of the skeletal muscle dihydropyridine receptor. *J. Biol. Chem.* 270, 22116-22118 (1995)
69. Casarotto,M.G., Green,D., Pace,S.M., Curtis,S.M. & Dulhunty,A.F. Structural determinants for activation or inhibition of ryanodine receptors by basic residues in the dihydropyridine receptor II-III loop. *Biophys. J.* 80, 2715-2726 (2001)
70. Murray,B.E. & Ohlendieck,K. Cross-linking analysis of the ryanodine receptor and ? $_1$-dihydropryidine receptor in rabbit skeletal muscle triads. *Biochem. J.* 324, 689-696 (1997)
71. Gurrola,G.B., Arevalo, C., Sreekkumar, R., Lokuta, A. J., Walker, J. W., Valdivia, H. H. Activation of ryanodine receptors by imperatoxin A and a peptide segment of the II-III loop of the dihydropyridine receptor. *J. Biol. Chem.* 274, 7879-7886 (1999)
72. Samso,M., Trujillo,R., Gurrola,G.B., Valdivia,H.H. & Wagenknecht,T. Three-dimensional location of the imperatoxin A binding site on the ryanodine receptor. *J. Cell Biol.* 146, 493-499 (1999)
73. El-Hayek,R., Lokuta,A.J., Arevalo,C. & Valdivia,H.H. Peptide probe of ryanodine receptor function. Imperatoxin A, a peptide from the venom of the scorpion *Pandinus imperator*, selectively activates skeletal-type ryanodine receptor isoforms. *J. Biol. Chem.* 270, 28696-28704 (1995)
74. Tripathy,A., Resch,W., Xu,L., Valdivia,H.H. & Meissner,G. Imperatoxin A induces subconductance states in Ca^{2+} release channels (ryanodine receptors) of cardiac and skeletal muscle. *J. Gen. Physiol.* 111, 679-690 (1998)
75. Yamazawa,T., Takeshima,H., Shimuta,M. & Iino,M. A region of the ryanodine receptor critical for excitation-contraction coupling in skeletal muscle. *J. Biol. Chem.* 272, 8161-8164 (1997)
76. Lu,X., Xu,L. & Meissner,G. Activation of the skeletal muscle calcium release channel by a cytoplasmic loop of the dihydropyridine receptor. *J. Biol. Chem.* 269, 6511-6516 (1994)
77. Trujillo,R., Liu, Z., Samso, M., Pattanyak, V., Pasek, D. A., & Meissner, G. Localization of Dihydropyridine Receptor II-III Loop:Ryanodine Receptor Interaction by Cryo-Electron Microscopy. (abstract) *Biophys. J.* 82, 76a (2002)
78. Treves,S., Chiozzi,P. & Zorzato,F. Identification of the domain recognized by anti-(ryanodine receptor) antibodies which affect Ca^{2+}-induced Ca^{2+} release. *Biochem. J.* 291, 757-763 (1993)
79. Benacquista,B.L., Sharma, M. R., Samso, M., Zorzato, F., Treves, S., & Wagenknecht, T. Amino acid residues 4425-4621 localized on the three-dimensional structure of the skeletal muscle ryanodine receptor. *Biophys. J.* 78, 1349-1358 (2000)
80. Moore,C.P., Zhang,J.-Z. & Hamilton,S.L. A role for cysteine 3635 of RYR1 in redox modulation and calmodulin binding. *J. Biol. Chem.* 274, 36831-36834 (1999)
81. Leong,P. & MacLennan,D.H. A 37-amino acid sequence in the skeletal muscle ryanodine receptor interacts with the cytoplasmic loop between domains II and II in the skeletal muscle dihydropyridine receptor. *J. Biol. Chem.* 273, 7791-7794 (1998)
82. Liu,Z., Zhang, J., Sharma, M. R., Li, P., Chen, S. R. W., & Wagenknecht, T. Three-dimensional reconstruction of the recombinant type 3 ryanodine receptor and localization of its amino terminus. *Proc. Natl. Acad. Sci. USA* 98, 6104-6109 (2001)
83. Yin,C.C. & Lai,F.A. Intrinsic lattice formation by the ryanodine receptor calcium-release channel. *Nature Cell Biology* 2, 669-671 (2000)
84. Matadeen,R., Patwardhan, A., Gowen, B., Orlova, E. V., Pape, T., Cuff, M., Mueller, F., Brimacombe, R. & van Heel, M. The *Escherichia coli* large ribosomal subunit at 7.5 Å resolution. *Structure* 7, 1575-1583 (1999)
85. Wriggers,W. & Birmanns,S. Using Situs for flexible and rigid-body fitting of multiresolution single-molecule data. *J. Struct. Biol.* 133, 193-202 (2001)
86. Volkmann,N. & Hanein,D. Quantitative fitting of atomic models into observed densities derived by electron microscopy. *J. Struct. Biol.* 125, 176-184 (1999)
87. Jiang,W., Baker,M.L., Ludtke,S.J. & Chiu,W. Bridging the information gap: Computational tools for intermediate resolution structure interpretation. *J. Mol. Biol.* 308, 1033-1044 (2001)
88. Kim,S., Shin,D.W., Kim,D.H. & Eom,S.H. Crystallization and preliminary X-ray crystallographic studies of the D2 region of the skeletal muscle ryanodine receptor. *Acta Crystallographica Section D-Biological Crystallography* 55, 1601-1603 (1999)

Abbreviations: 3D, three-dimensional, CaM, calmodulin; CRU, calcium release unit; DHPR, dihydropyridine receptor; E-C, excitation-contraction; EM, electron microscopy; FKBP, FK506-binding protein; $IpTx_a$, imperatoxin A; RyR, ryanodine receptor; SR, sarcoplasmic reticulum; T-tubule, transverse tubule.

Key Words: Ryanodine Receptor, Dihydropyridine Receptor, Excitation-Contraction Coupling, FKBP, Calmodulin, Imperatoxin A, 3D Reconstruction, Cryo-Electron Microscopy, Image Processing, Review

Send correspondence to: Dr. T. Wagenknecht, Biggs Laboratory, Wadsworth Center, New York State Department of Health, Albany, NY 12201, Tel:518-474-2450, Fax: 518-474-7992; E-mail: tcw02@wcnotes.wadsworth.org